Transmission resonances in a semiconductor-superconductor junction quantum interference structure

Y. Takagaki and Y. Tokura
NTT Basic Research Laboratories, Atsugi, Kanagawa 243-01, Japan
(Received 12 February 1996; revised manuscript received 15 May 1996)

Transport properties in a quantum resonator structure of a normal-conductor–superconductor (NS) junction are calculated. Quasiparticles in a cavity region undergo multiple reflections due to an abrupt change in the width of the wire and the NS interface. Quantum interference of the reflections modulates the nominal normal reflection probability at the NS boundary. We show that various NS structures can be regarded as the quantum resonator because of the absence of propagation along the NS interface. When the incident energy coincides with the quasibound state energy levels, the zero-voltage conductance exhibits peaks for small voltages applied to the NS junction. The transmission peaks change to dips of nearly perfect reflection when the applied voltage exceeds a critical value. Two branches of the resonance, which are roughly characterized by electron and hole wavelengths, emerge from the individual dip, and the energy difference between them increases with increasing voltage. The electronlike and holelike resonance dips originating from different quasibound states at zero-voltage cross one after another when the voltage approaches the superconducting gap. We find that both crossing and anticrossing can be produced. It is shown that the individual resonance state in the NS system is associated with two zeros and two poles in the complex energy plane. The behavior of the resonance is explained in terms of splitting and merging of the zero-pole pairs. We examine the Green's function of a one-dimensional NS system in order to find out how the transmission properties are influenced by the scattering from the NS interface. [S0163-1829(96)08033-2]

I. INTRODUCTION

The energy spectrum in a quantum dot comprises discrete energy levels.[1] When narrow leads are attached to the dot, an electron can be injected from the lead to the states in the dot (unless this injection is forbidden because of the parity of the wave function[2]) whenever the incident energy coincides with the discrete levels. The mixing of the lead state and the confined state induces a dip[3] or a peak[2] in the transmission through the structure. The transmission resonance results in the dip when the coupling is sustained by a propagating mode, whereas it turns out to be the peak if an evanescent mode is responsible for the coupling.[2,4] The states in the dot which can be accessed by the incident electron are hence quasibound states rather than true bound states. The strength of the coupling between the lead and dot states determines the decay time $\tau=\hbar/\Gamma$ of the quasibound state,[5] which is related to the resonance width of the Lorentzian line shape of the transmission probability $T(E)$:

$$T(E)=\frac{\Gamma^2/4}{(E-E_p)^2+\Gamma^2/4}. \tag{1}$$

In fact, it has been confirmed that two electrons are added to the system[6] when the Fermi energy increases by $\sim\Gamma$ around E_p. The factor 2 arises from spin degeneracy. Porod, Shao, and Lent[7] have shown that the transmission resonance in quantum waveguides is characterized by a pair of a pole and a zero in the complex energy plane, whereas that in resonant tunneling structures induces only a pole. In this interpretation, Γ is the distance between the pole and the real energy axis.[8]

Recent experiments on electron transport in nanostructures fabricated in a normal-conductor–superconductor (NS) junction have uncovered another aspect of quantum-mechanical effects in mesoscopic systems. By employing a high-mobility two-dimensional electron gas in an InAs channel inserted into InGaAs-InAlAs heterostructures as the normal conductor, the transport in the normal region can be made ballistic.[9] The quantum transport phenomena in semiconductor wires and dots that originate from the wave nature of an electron are modified significantly in the NS system due to the unusual reflection of quasiparticles from the NS interface known as Andreev reflection.[10] The current in the bulk of the superconductor is carried by Cooper pairs. As a consequence, an electronlike excitation injected from a semiconductor with the energy slightly above the Fermi energy μ is reflected from the NS interface as a holelike excitation with the energy slightly below μ in order to satisfy the charge conservation across the interface.[11] The wave function of these unpaired quasiparticles decays in the superconductor whenever the excitation energy ε is smaller than the pair potential amplitude Δ. The phase-coherent transport of the quasiparticles in the NS system is described by the Bogoliubov–de Gennes (BdG) equation[12]

$$\begin{pmatrix} H & \Delta(x,y) \\ \Delta^*(x,y) & -H^* \end{pmatrix}\begin{pmatrix} u \\ v \end{pmatrix}=\varepsilon\begin{pmatrix} u \\ v \end{pmatrix}, \tag{2}$$

where $u(x,y)$ and $v(x,y)$ are electron and hole wave functions and $H=[p+eA]^2/2m+U(x,y)-\mu$ is the single-particle Hamiltonian with $U(x,y)$ and $A(x,y)$, respectively, being the electrostatic and vector potentials.

In this paper, the transmission resonance in a quantum waveguide structure containing the NS junction is investi-

gated. It has been demonstrated that remarkable features are evident in the transport properties of mesoscopic NS systems because of the simultaneous presence of the quantum interference effects and Andreev reflection.[13,14] The phase-coherent Andreev reflection was first studied by Beenakker.[13] When the voltage $V=\varepsilon/e$ applied to the NS junction is small, the interference effect enhances the transmission due to the retroproperty of Andreev reflection. In this sense, the resonance in the NS quantum resonator results in a peak. The modification is hence visible if the normal reflection probability at the NS junction is sufficiently large. The conductance exhibits a periodic modulation as a function of the chemical potential or the sample dimension when large normal reflection is achieved, for instance, by increasing the difference between the chemical potentials in the semiconductor and the superconductor. A prominent feature of the interference effects in the NS system is revealed when the applied voltage is increased due to breakdown of the retroproperty. The behavior of the resonance changes suddenly when eV becomes appreciable compared to the superconducting gap energy Δ. The transmission peak changes rapidly to a dip when eV is varied over a small range just below ε_c, drops to zero at $eV=\varepsilon_c$, and splits into two dips for $eV>\varepsilon_c$. As eV approaches Δ, the positions of the dips in energy diverge symmetrically with respect to the original peak position. It is found that the zero-pole pair in the complex energy plane is actually a combination of two quasi-zero-pole pairs, each of which is attributed to the electronlike and holelike excitations and are therefore degenerate when $\varepsilon=0$. In contrast to the zero-pole pair in the semiconductor waveguide structures, the zeros and poles in the NS waveguide structures are not always complete: the transmission probability neither becomes zero nor diverges when V is small. In addition, the zeros in the NS system need not be on the real energy axis. Since the resonance is characterized by the two kinds of zero-pole pairs and the energy levels have opposite V dependence, coincidence of the electronlike and holelike transmission dips originating from various quasi-bound states occurs while eV is swept up to Δ. It will be shown that crossing and anticrossing of the resonance show up in the transmission depending on the choice of the sample parameters. These complicated behaviors of the resonance becomes possible because of the flexibility of the zeros in the NS system.

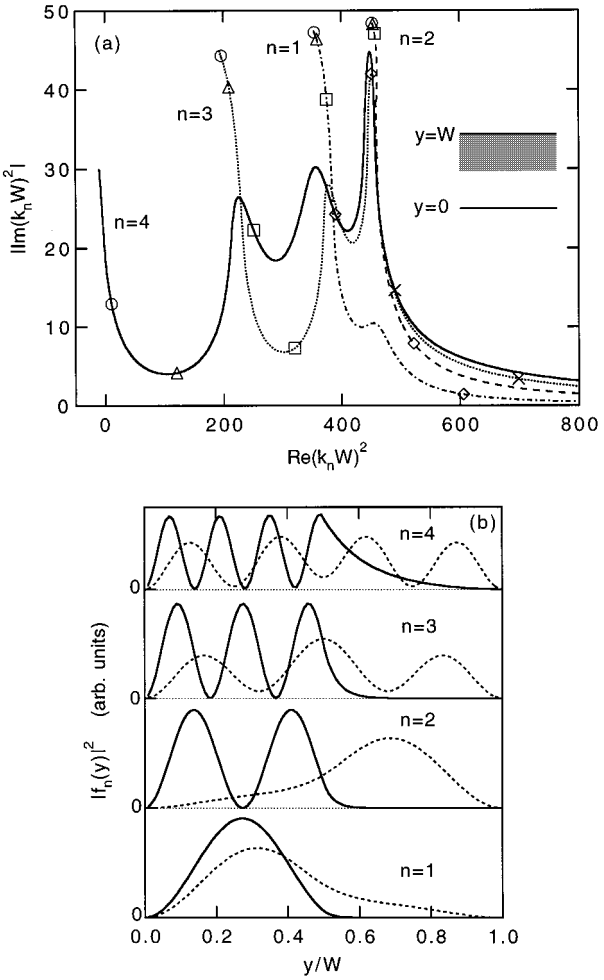

FIG. 1. (a) Real and imaginary parts of $(k_nW)^2$ for $n=1-4$ as a function of chemical potential μ_N in the normal-conductor when $\varepsilon=0$. Circles, triangles, squares, diamonds, and crosses indicate the positions for $\mu_N/E_1=4$, 16, 36, 64, and 100, respectively. Inset: The shaded area represents the superconducting region. (b) Probability distribution when $\mu_N/E_1=49$ (dotted lines) and 100 (solid lines). The squared amplitude is identical for the electron and the hole as $\varepsilon=0$.

II. TRANSMISSION MODES ALONG THE NS INTERFACE

Before evaluating the transmission resonances in the NS system, we examine transmission modes moving parallel to the NS interface. The semiconductor-superconductor junction quantum point contact (QPC) used in the experiments in Ref. 9 possesses multiterminal geometry, i.e., the two-dimensional electron gas sandwiched by the split gate and the NS interface extends longer than the phase coherence length in the direction perpendicular to the current flow. The purpose of this section is to show that there exists no propagating mode traveling parallel to the NS interface provided that the Andreev reflection probability is not too small. Thus, the superconducting-QPC-type devices are practically regarded as two-terminal structures if inelastic scattering is negligible, which is also a criterion to observe the quantum interference effect. The phenomena we investigate in the present paper are of significant importance in the superconducting QPC as well.

Consider the composite NS wire illustrated in the inset of Fig. 1. The normal-conductor and superconductor parts are assumed to have the same width $W/2$. We set a uniform pair potential[15] Δ_0 in the superconductor ($W/2<y<W$), whereas $\Delta(x,y)=0$ is imposed in the semiconductor ($0<y<W/2$). We wish to find a solution to Eq. (2) of the separable form

$$\begin{pmatrix} u(x,y) \\ v(x,y) \end{pmatrix} = e^{ikx} \begin{pmatrix} f(y) \\ g(y) \end{pmatrix}. \tag{3}$$

If the wire consists entirely of the superconductor, the wave numbers k_n^+ and k_n^- for the electron and the hole are given by

$$\frac{\hbar^2 k_n^{\pm 2}}{2m} = \mu - E_n \pm i\sqrt{\Delta_0^2-\varepsilon^2}, \tag{4}$$

where $E_n=(n\pi\hbar/W)^2/2m$ is the threshold energy of the nth mode. Therefore, propagating modes are not allowed in the superconductor when $\varepsilon<\Delta_0$. To determine the wave number k and the wave functions $f(y)$ and $g(y)$ in the composite system, we approximate the wire by a square lattice with lattice constant a. The BdG equation reduces to the equation of motion[16]

$$(\varepsilon-H_0)C_l+tPC_{l-1}+tP^*C_{l+1}=0, \tag{5}$$

where $t=\hbar^2/2ma^2$ is the transfer integral. In the absence of a magnetic field, the $2M\times 2M$ diagonal matrix P is given by $P_{ii}=1$ for $i=1,\ldots,M$ and $P_{ii}=-1$ for $i=M+1,\ldots,2M$. Here M is the number of lattice sites in the transverse direction. The wave function in the lth slice is represented by C_l as

$$C_l=\begin{pmatrix} u_l \\ v_l \end{pmatrix}. \tag{6}$$

The Hamiltonian matrix H_0 is given by

$$H_0=\begin{pmatrix} H_a & H_b \\ H_b & -H_a \end{pmatrix}, \tag{7}$$

where

$$H_a=\begin{pmatrix} 4t-\mu & -t & 0 & \cdots & 0 \\ -t & 4t-\mu & -t & \cdots & 0 \\ 0 & -t & 4t-\mu & \cdots & 0 \\ \vdots & \vdots & \vdots & \ddots & \vdots \\ 0 & 0 & 0 & \cdots & 4t-\mu \end{pmatrix}, \tag{8a}$$

$$(H_b)_{ij}=\begin{cases} \Delta_0, & i=j=M/2+1,\ldots,M, \\ 0, & \text{otherwise.} \end{cases} \tag{8b}$$

Using $C_l=\lambda C_{l-1}$ with $\lambda=e^{ika}$, it is shown that the transmission modes in the NS wire are obtained as linear independent solutions of the following eigenvalue problem:

$$\begin{pmatrix} t^{-1}P(H_0-\varepsilon) & -P^2 \\ 1 & 0 \end{pmatrix}\begin{pmatrix} C_l \\ C_{l-1} \end{pmatrix}=\lambda\begin{pmatrix} C_l \\ C_{l-1} \end{pmatrix}. \tag{9}$$

The value $(k_nW)^2$ in the composite NS wire is plotted in Fig. 1(a) as a function of the chemical potential $\mu_N=\hbar^2k_F^2/2m$ in the normal conductor when $\varepsilon=0$. We have assumed a constant chemical potential $\mu_S=49E_1$ and $\Delta_0=0.1\mu_S$ in the superconductor. On the one hand, $(k_nW)^2$ is real in a semiconductor (i.e., when $\Delta_0=0$), and is greater than zero for propagating modes and less than zero for evanescent modes. On the other hand, $(k_nW)^2$ is complex[17] in the superconductor when $\varepsilon<\Delta_0$. Nevertheless, the curves in Fig. 1(a) would be parallel to the real axis if the system were made of solely a semiconductor or solely a superconductor. The imaginary part of $(k_nW)^2$ in the composite wire, however, fluctuates as μ_N varies. Although μ_N is large enough to be able to afford propagating modes if the wire is divided at the NS interface, all the modes are generally found to be evanescent modes due to the strong proximity effect of the superconductor. The absence of the propagating modes moving parallel to the NS junction is explained in terms of the retroreflection at the interface. Suppose that a quasiparticle is incident from the left-hand side in the positive x direction, the retroproperty of Andreev reflection compels the quasiparticle scattered at the NS interface to trace back the trajectory along which it arrived. Because all the quasiparticles are eventually Andreev reflected into the source in an infinite wire, propagating modes cannot survive whenever Andreev reflection predominates over the normal reflection (see Appendix A). For μ_N considerably larger than μ_S, the normal reflection is enhanced and $(k_nW)^2$ of the lower modes therefore approaches the real axis. We find that, for the parameters used in Fig. 1, the lowest mode becomes a propagating mode when $\mu_N>223E_1$. In the opposite limit $\mu_N\to 0$, the real part of $(k_nW)^2$ converges to certain values ζ_n, which Eq. (4) implies are related to the threshold energy. When the $\mathrm{Re}(k_nW)^2$ of higher-lying modes takes values close to ζ_m (generally $m<n$), $\mathrm{Im}(k_nW)^2$ shows peaks that remind us of the enhancement of scattering at the mode thresholds.[18]

The probability distribution of the four lowest modes is shown in Fig. 1(b) for $\varepsilon=0$. Because of the large penetration length $\xi\equiv\hbar k_F/2m\Delta_0=0.45W$ in the superconductor, the wave function extends into the superconducting region significantly when $\mu_N=\mu_S$. The penetration of the wave function in the superconductor decreases with increasing Δ_0. Equations (2) and (3) indicate that $g(y)=if(y)$ when $\varepsilon=0$. Under this circumstance, the Sturn-Liouville analysis of the BdG equation reveals that the wave functions $f_n(y)$ satisfy

$$(k_m^{2*}-k_n^2)\int_0^W f_m^*(y)f_n(y)dy = i\,\frac{4m}{\hbar^2}\int_0^W \Delta(y)f_m^*(y)f_n(y)dy. \tag{10}$$

If the pair potential amplitude is independent of y, the wave functions are orthogonal whenever $m\neq n$. Note that it can be also shown that

$$(k_m^2-k_n^2)\int_0^W f_m(y)f_n(y)dy=0. \tag{11}$$

In general, the value ζ_n is smaller for larger n. However, $\zeta_2>\zeta_1$ in Fig. 1(a) because the $n=2$ mode has an unusual character, i.e., the quasiparticle is predominantly located in the superconducting region. The wave functions for $n=1$ and 2 resemble one another. It is anticipated that the interaction between the two lowest modes produces anticrossing of the dispersion curves, which can account for the exchange of the mode index in the limits of large and small μ_N. When μ_N is increased relative to μ_S, the wave function localizes in the normal-conductor region. The lower modes eventually be-

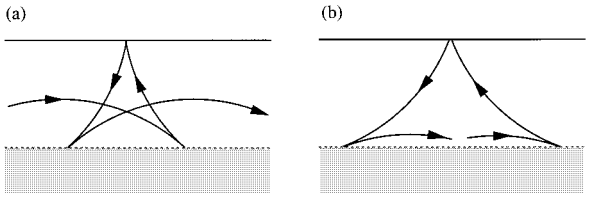

FIG. 2. Classical trajectories that propagate in the (a) forward and (b) backward direction along the NS interface.

come propagating modes for $\mu_N \gg \mu_S$ because of the increased normal reflection at the NS interface.

In the presence of a magnetic field B the Andreev-reflected quasiparticles no longer return to the current source, and propagating modes are therefore expected to appear as suggested by the classical trajectories shown in Fig. 2. If we assume that the magnetic field vanishes in the superconducting region, we can choose a gauge such that $A=[-B(y-W/2),0,0]$ for $y<W/2$ and $A=0$ for $y>W/2$. The matrix P acquires a phase shift due to the vector potential as

$$P_{jj}=\begin{cases} \exp[2\pi i\nu(j-M/2-1/2)] & (j=1,\ldots,M/2), \\ 1 & (j=M/2+1,\ldots,M), \\ -\exp[-2\pi i\nu(j-3M/2-1/2)] & (j=M+1,\ldots,3M/2), \\ -1 & (j=3M/2+1,\ldots,2M), \end{cases} \tag{12}$$

where $\nu=Ba^2/(h/e)$ is the number of flux quanta per unit lattice area. Figure 3 shows $\kappa_n W=-(M+1)\ln|\lambda_n|$, where $\kappa_n=\mathrm{Im}\,k_n$, as a function of $\hbar\omega_c/\mu_N$ for $\mu_N=\mu_S=49E_1$ and $\Delta_0=0.3\mu_S$. The lower modes become propagating ones when a weak magnetic field is applied. The higher modes require larger B to propagate. The threshold energies are lifted above the Fermi energy in strong magnetic fields, and so the propagating modes again become evanescent modes when $\hbar\omega_c \gg \mu_N$. As shown in Fig. 3(a), the $n=2$ and 3 modes temporarily become evanescent modes when $\hbar\omega_c/\mu_N \sim 0.03$. This transition ceases as the penetration of the wave function into the superconductor is reduced by increasing Δ_0, suggesting that it is due to a boundary-related interference in the superconductor.

III. TRANSMISSION RESONANCES IN A NS WAVEGUIDE STRUCTURE

We now examine the transmission resonances in the NS quantum resonator structure depicted in Fig. 4. The device is composed of a narrow normal-conductor wire with the width W, a normal-conductor cavity with the width D and the length L, and a wide superconductor wire lead with the width D. A quasiparticle incident from the narrow wire is reflected between the narrow-wide (NW) junction and the NS junction. Transmission properties in a narrow-wide-narrow (NWN) quantum wire structure (or often referred as the T-shaped transistor[3]) have been investigated extensively to study the quantum interference effects in the semiconductor nanostructures and also to evaluate the possibility of device application of the interference effects. The scattering from the NW junctions creates quasibound states in the wide region. Transmission through the NWN structure exhibits sharp resonance dips when the incident energy of an electron coincides with the quasibound state levels.[6,19] In comparison with the T-shaped transistor, one of the NW junctions is replaced by the NS junction. The quasibound states (weakly confined states in the cavity region) appear in the NS structure because the effective potential for the quasiparticles in the cavity region is lower than that in the narrow normal lead, due to the transverse confinement, and in the superconductor, due to the superconducting gap. The interference of the reflections is anticipated to dominate the transmission characteristics of the NS structure when the sample dimensions are comparable to the wavelength. As we consider the case in which the voltage V applied to the NS junction is smaller than Δ_0/e, the quasiparticles injected from the semiconductor are completely reflected (either as a hole or as an electron) by the superconductor. Therefore, the two-terminal conductance of the device is given by[20,21]

$$G_{\mathrm{NS}}=\partial I_{\mathrm{NS}}/\partial V=(2e^2/h)\mathrm{Tr}(1-s_{ee}s_{ee}^{\dagger}+s_{he}s_{he}^{\dagger})$$

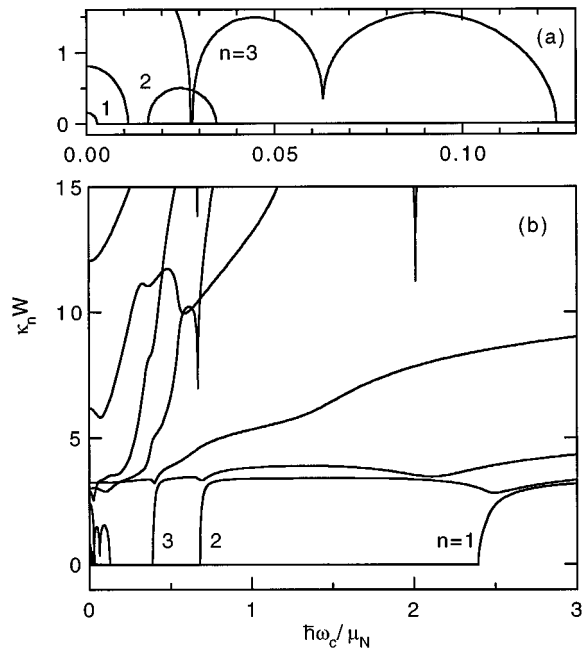

FIG. 3. Imaginary part of the wave number $\kappa_n W=\mathrm{Im}k_n W=-(M+1)\ln|\lambda_n|$ as a function of $\hbar\omega_c/\mu_N$.

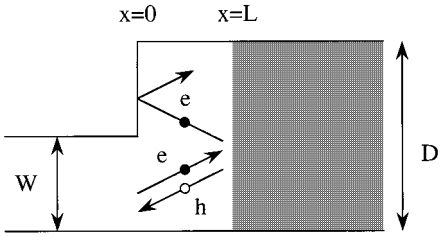

FIG. 4. Schematic of semiconductor-superconductor quantum interference structure. The shaded area represents the superconducting region. An electron (e) is scattered from the superconductor in part as a hole (h) and the remainder as an electron.

$$=(4e^2/h)\mathrm{Tr}(s_{he}s_{he}^{\dagger}), \tag{13}$$

where s_{he} (s_{ee}) describes the scattering amplitude for a particle incident as an electron from the left-hand side lead and reflected as a hole (an electron) in the same lead. One notices that the conductance is quantized at values twice those in the semiconductor if the electron is perfectly Andreev reflected.[13] The holes supplied by the NS interface generate a current that is identical in magnitude to that generated by the initially injected electrons. The resultant increase of the total current I_{NS} is responsible for the doubling of the quantized conductance unit. The scattering matrix can be determined using the lattice Green's-function technique or the modal expansion method. For the lattice Green's-function technique, the reflection amplitudes s_{he} and s_{ee} are obtained using the technique developed by Ando.[16] For the modal expansion method, the structure is divided into three waveguide segments: $x<0$, $0<x<L$, and $x>L$. The wave function when an electron is injected through mode n is obtained as a superposition of the standing wave solutions in each portion:[12,22]

$$\Psi_n(x,y)=\begin{cases}\begin{pmatrix}1\\0\end{pmatrix}e^{ik_n^{+}x}f_n(y)+\sum_m\left[\begin{pmatrix}1\\0\end{pmatrix}A_{mn}e^{-ik_m^{+}x}+\begin{pmatrix}0\\1\end{pmatrix}B_{mn}e^{ik_m^{-}x}\right]f_m(y) & (x\leqslant 0),\\ \sum_m\left[\begin{pmatrix}1\\0\end{pmatrix}\{C_{mn}e^{iq_m^{+}x}+D_{mn}e^{-iq_m^{+}x}\}+\begin{pmatrix}0\\1\end{pmatrix}\{E_{mn}e^{-iq_m^{-}x}+F_{mn}e^{iq_m^{-}x}\}\right]g_m(y) & (0\leqslant x\leqslant L),\\ \sum_m\left[\begin{pmatrix}\varphi\\ \phi\end{pmatrix}G_{mn}e^{ip_m^{+}x}+\begin{pmatrix}\varphi\\ \phi^{*}\end{pmatrix}H_{mn}e^{-ip_m^{-}x}\right]g_m(y) & (\geqslant L),\end{cases} \tag{14}$$

where

$$\varphi=\frac{1}{\sqrt{2}},\quad \phi=\frac{\varepsilon-i\sqrt{\Delta_0^2-\varepsilon^2}}{\sqrt{2}\Delta_0}. \tag{15}$$

The sign of the wave numbers in the superconductor is defined as summarized in Table I. The imaginary part is chosen to express the decaying wave, whereas the real part represents opposite phase shifts for the electron and the hole. The unknown coefficients $A_{mn}, B_{mn}, \ldots H_{mn}$ are evaluated by imposing the continuity of the wave function and its normal derivative at the interfaces[23] at $x=0$ and L. The reflection amplitudes are given by

$$(s_{ee})_{mn}=(k_m^{+}/k_n^{+})^{1/2}A_{mn}, \tag{16a}$$

$$(s_{he})_{mn}=(k_m^{-}/k_n^{+})^{1/2}B_{mn}. \tag{16b}$$

Figure 5 shows G_{NS} as a function of D/W for several values of the ratio μ_S/μ_N of the chemical potentials in the superconductor and the normal-conductor. Since $\Delta_0 \ll \mu$, almost all the electrons are Andreev-reflected at the NS interface,[11] resulting in a nearly complete conductance doubling when $D=W$. We expect a modulation to appear in the conductance due to the scattering from the NW junction with increasing D. A dip in G_{NS} may be anticipated in analogy to the NWN structure.[3] It is found, however, that the conductance remains almost unchanged at $4e^2/h$ when $\mu_S=\mu_N$ (see the topmost curve in Fig. 5). The nominal absence of the scattering from the NW junction arises from the retroproperty of Andreev reflection. The Andreev-reflected holes exactly trace back the trajectories along which the electrons arrived. Consequently, they enter the narrow lead without being scattered by the NW junction in the classical limit. The reflectionless transmission, in general, does not take place in a quantum-mechanical situation. Nevertheless, the scattering from the NW junction is much less effective compared with that for the normally reflected electrons. In experimental devices, the normal reflection probability is considerably large because of the difference of the Fermi energies in the semiconductor and the superconductor. The presence of a roughness or a potential barrier at the NS interface also enhances

TABLE I. The sign of k_n^2 is set as listed below. Here, ρ, $\sigma>0$. We use the definition of square root such that $\mathrm{Im}\,k_n>(<)0$ when $\mathrm{Im}\,k_n^2>(<)0$.

	Propagating modes	Evanescent modes
Electron	$\rho+i\sigma$	$-\rho+i\sigma$
Hole	$\rho-i\sigma$	$-\rho-i\sigma$

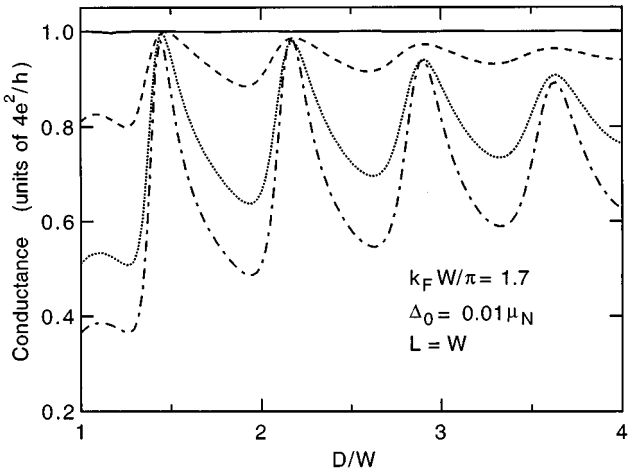

FIG. 5. Conductance as a function of the ratio D/W of the widths of the semiconductor region. The ratio μ_S/μ_N of the Fermi energies in the superconducting and normal regions is 1, 2, 4, and 6 for the curves from top to bottom.

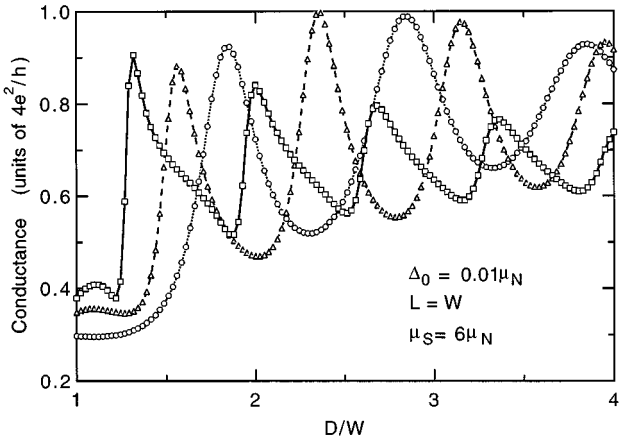

FIG. 6. Period of the oscillation in D decreases when the Fermi wavelength becomes shorter. The circles, triangles, and squares show the conductance when $k_F W/\pi = 1.4$, 1.6, and 1.8, respectively.

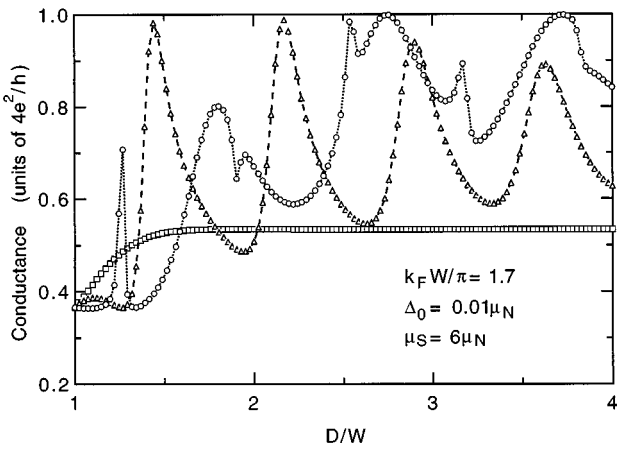

FIG. 7. The oscillation disappears when $L = 0.5W$ (squares) as the quasiparticle wave functions do not penetrate the wide semiconductor region in the transverse direction. The resonance line shape becomes complicated when $L = 1.5W$ (circles) as more than one mode are available for the interference. The triangles indicate the conductance when $L = W$.

the normal reflection probability.[12,22,24] The conductance of the NS junction when the Fermi energy μ_S in the superconductor is increased relative to that (μ_N) in the normal-conductor indicates that a periodic oscillation shows up in the D dependence of $G_{\rm NS}$ as the conductance is reduced by enhancing the normal reflection at the NS boundary. The normal reflection caused by the difference in μ can be suppressed almost completely by tuning D. The peaks in the D dependence are broader in the NS structure than the dips in the NWN structure, which are characterized by the Breit-Wigner formula.[6] The reflectionless tunneling through a barrier and the non-Lorentzian line shape of the resonance in the NS system were first derived by Beenakker.[10,13] Although the oscillation resembles the conductance modulation in the NWN structure, the appearance of the interference effect is contrary in the NS structure. The resonances result in dips in the transmission in the semiconductor device.[3,6,19] Instead, peaks are achieved in the NS device. In contrast to the Andreev-reflected holes, the normal-reflected electrons undergo multiple reflections in the wide region, and so the interference effect plays an important role in the transmission of these electrons. Since the normal reflection reduces the conductance, the interference in the normal reflection process results in the increase of the conductance. Alternatively, one may interpret this as indicating that the interference of the hole always occurs as the phase shift cancels out along the Andreev-reflected path.[25]

The conductance is plotted in Fig. 6 for different Fermi wavelengths. The period of the oscillation becomes smaller with decreasing wavelength. In fact, we find that the peaks appear whenever the condition

$$(i+C)\lambda_1/2 = D, \quad i = 1,2, \ldots, \tag{17}$$

is satisfied as has been known for the resonances in the NWN structure. Here, C is a constant and

$$\lambda_n/W = 2[(k_F W/\pi)^2 - (nW/L^*)^2]^{-1/2} \tag{18}$$

is the wavelength of the nth mode in the wide region in the transverse direction. Despite the large penetration depth of quasiparticles into the superconductor, $\xi = 185W$ for Fig. 6, we find that $L^* \approx L$. When the Fermi energy approaches the threshold of the second mode, the shape of the oscillation becomes highly distorted due to the proximity effect of the second mode.

Figure 7 shows the conductance for $L/W = 0.5$, 1.0, and 1.5. We find that the period in D/W becomes large when L is decreased (not shown) according to Eq. (18). The wave function cannot penetrate in the transverse direction when $L = 0.5W$, and so the oscillation vanishes. On the other hand, the oscillation becomes complicated and sharp peaks and dips emerge when $L > W$ since multiple modes contribute to the oscillations. Therefore, the clearest oscillation suitable for a device application is produced when $L = W$. These behaviors are similar to those found for the oscillations in the NWN structure.[26] Therefore, we assume $L = W$ throughout the remainder of the paper. Notice that, although the conductance modulation resembles that in the resonant tunneling structure, the maximum conductance does not necessarily become unity at the resonances.

We have so far considered the case of infinitesimal voltage. We show $G_{\rm NS}$ in Fig. 8 as functions of $k_F W/\pi$ and eV/Δ_0 for $\mu_S = 13E_1$ and $\Delta_0 = 0.02\mu_S$. The wave numbers k_n^+ and k_n^- in the normal conductor are given by

$$k_n^{\pm} = (2m/\hbar^2)^{1/2}(\mu_N - E_n \pm eV)^{1/2}. \tag{19}$$

With increasing eV, the threshold of the hole channels moves higher in energy. The conductance is hence zero at the upper right corners in Fig. 8 because the electron is completely normal reflected. Similarly, the threshold energy of the electron channels decreases, producing singularities[27] at $k_F W/\pi \approx 2 - eV/4E_1$. The single periodicity observed when $V = 0$ may be expected to split into two oscillations associated with the electronlike and holelike wave numbers. However, we find that simple splitting of the periodicity for the conductance peaks is not what happens. The peak conductance initially increases and becomes closer to unity for larger eV. The situation then changes drastically when

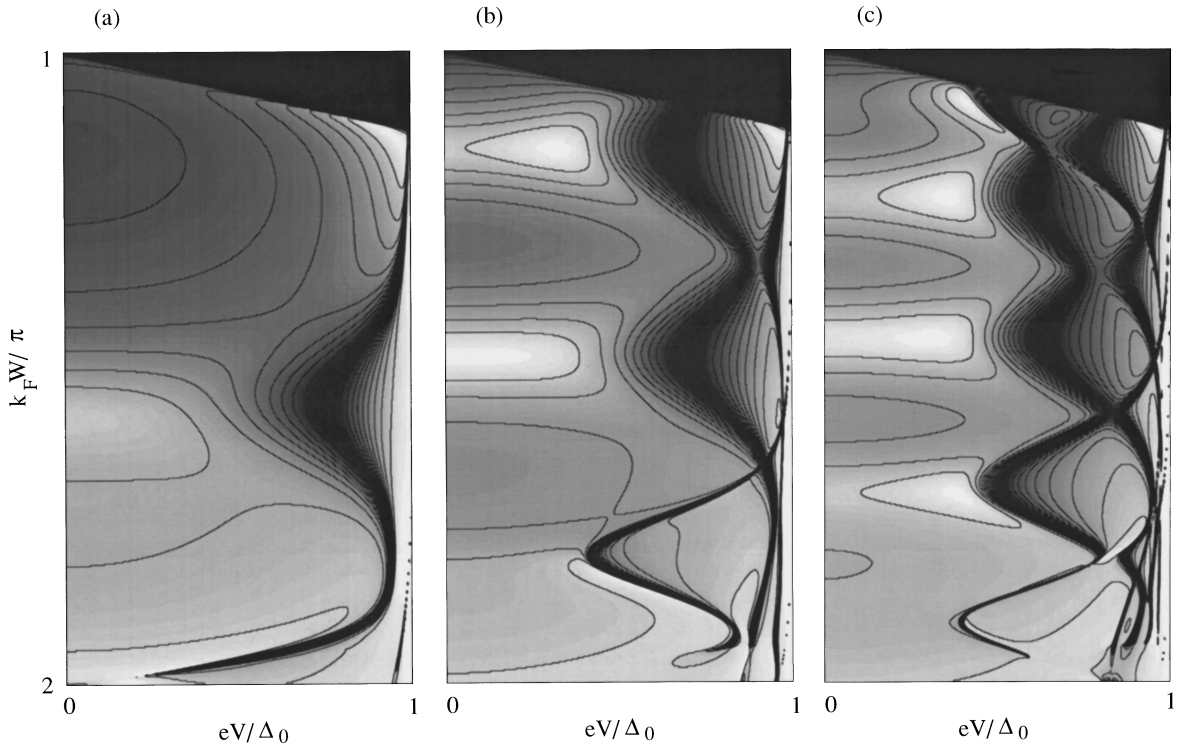

FIG. 8. Conductance G_{NS} as functions of Fermi wave number k_F in the normal-conductor and applied voltage V for $D/W=$(a) 1.6, (b) 2.6, and (c) 3.6. More conductive areas are brighter.

$eV\sim\Delta_0/2$. The conductance modulation reveals complicated structures with increasing V as shown in Figs. 9 and 10. The peaks suddenly turn into dips (as evidenced by the dotted line in Fig. 9 at $k_F W/\pi=1.15$ and 1.48). The conductance at the bottom of these dips diminishes until it becomes zero at a critical value $eV=\varepsilon_c$ with the position in $k_F W/\pi$ or D/W nearly unchanged. As a consequence of the sharp dips that emerge when $eV\neq\Delta_0$, a significant conductance modulation as a function of $k_F W/\pi$ or D/W is obtained when eV approaches Δ_0 even for $\mu_S=\mu_N$, which is in contrast to the almost invisible modulation when $V=0$. Beyond ε_c the dip splits into two narrow dips, which are typical in NWN quantum resonator structures. The branching occurs at lower voltages for the resonances at larger D/W. According to Eq. (19), the Fermi wavelength of the electron becomes shorter for larger eV, whereas that of the hole becomes longer. Therefore, each dip is ascribed to the interference of the electronlike and holelike quasiparticles. The position of the dips are satisfactorily described by Eqs. (17)–(19). The distance between the dips in energy diverges as eV approaches the superconducting gap Δ_0. In the presence of the applied voltage, the retroproperty of Andreev reflection breaks down. As a consequence, both the normal-reflected electron and the Andreev-reflected hole experience multiple reflection in the cavity region and contribute to the resonance. As we are dealing with the regime $eV<\Delta_0$, the influence of the applied voltage is significant when Δ_0/μ_N is large. Assuming the superconducting gap of Nb (1.5 meV)[9] and the effective mass in GaAs, the sheet electron density corresponding to $\Delta_0=0.1\mu_N$ is 4.2×10^{15} m^{-2}, which is a typical value in GaAs-AlGaAs heterostructures.

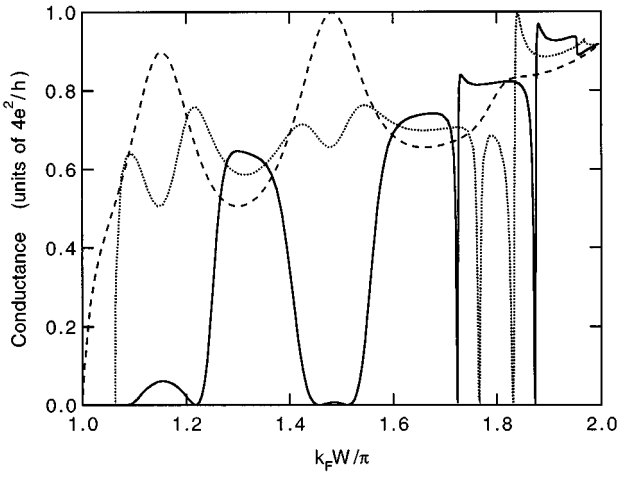

FIG. 9. Conductance G_{NS} as a function of $k_F W/\pi$ for $D=2.6W$, $\mu_S=13E_1$ and $\Delta_0=0.02\mu_S$. The applied voltages for the dashed, dotted, and solid lines are $eV/\Delta_0=0$, 0.5, and 0.7, respectively.

When the dips originating from different quasibound states at $V=0$ cross each other, both crossing and anticrossing can be found to take place. The expanded plots shown in Fig. 11 demonstrate the transition between the crossing and the anticrossing. The resonances shift to lower energies as D is increased. Typical shapes at the crossing point can be found in Fig. 8(b). The anticrossing at $k_F W/\pi=1.9$ becomes the crossing like at $k_F W/\pi=1.6$, and then again the anticrossing like at $k_F W/\pi=1.3$. The first dip below the threshold of the second mode is always distinctively narrow compared with the resonances at lower energies. One might suspect that the narrow resonance is of different origin. We find, however, that the sharp dip becomes broad like the rest

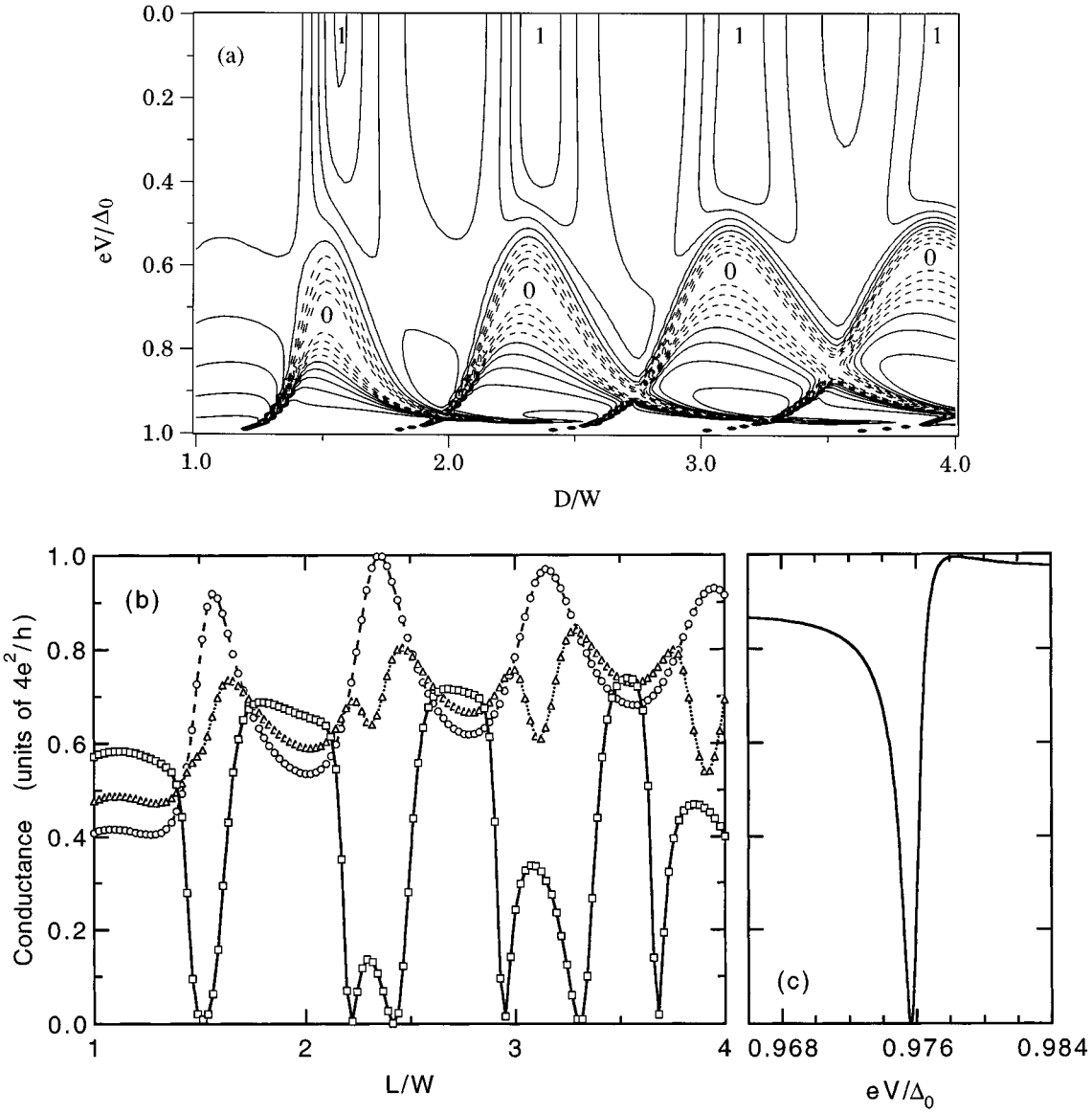

FIG. 10. Conductance when nonzero voltages are applied to the junction for $k_F W/\pi=1.6$, $\Delta_0=0.1\mu_N$, $\mu_S=5\mu_N$, and $D=W$. With increasing the voltage, the resonance peaks become sharp dips and then the dips split into two branches associated with electron and hole. (b) Slices of the contour plot. The applied voltage is $eV/\Delta_0=0.0$, 0.5, and 0.7 for the circles, triangles, and squares, respectively. (c) Conductance as a function of the applied voltage when $D/W=1.27$.

of the resonances when D is extended to yield another dip just below the threshold of the second mode.

When the applied voltage is sufficiently close to Δ_0/e, it is often found that the resonant reflection shows Fano-type line shape as shown in Figs. 9 and 10(c), i.e., a peak occurs subsequently after the dip at a small separation. It has been established that the transmission resonance in the NWN structure gives rise to a zero-pole pair of the transmission coefficient in the complex energy plane.[7,28] As a consequence, the resonance peak and dip and also the doublet combination of them can be produced depending on the position of the transmission pole in the complex energy plane. It has been identified that the form of the transmission amplitude is $t(E)\sim(E-E_z)/[E-(E_p-i\Gamma)]$, which yields the Lorentzian-shaped dip in the transmission probability in a special case.[28] In the semiconductor waveguide, zeros always appear on the real energy axis, whereas this is obviously not always what happens in the NS waveguide.

To investigate the transmission poles in the NS system, the conductance is shown in Figs. 12 and 13 in the complex energy plane, $E=\mu N+iE_i$. Although the conductance at the complex energies may not have an immediate physical sense, the formal method has been demonstrated to be useful to analyze the transmission resonances as it provides the life time of the quasibound states.[7,8,28,29] As suggested by the Fano-type behavior, the conductance zero accompanies a pole.[7] In the NS waveguides, the conductance is actually featureless when $V=0$ in the complex energy plane. Quasi-zero-pole pairs are created as V is increased. In contrast to what is seen in the semiconductor waveguides, the zero-pole pairs are not fully developed for small V. The conductance does not drop to zero at the ''zeros'' nor does it diverge at

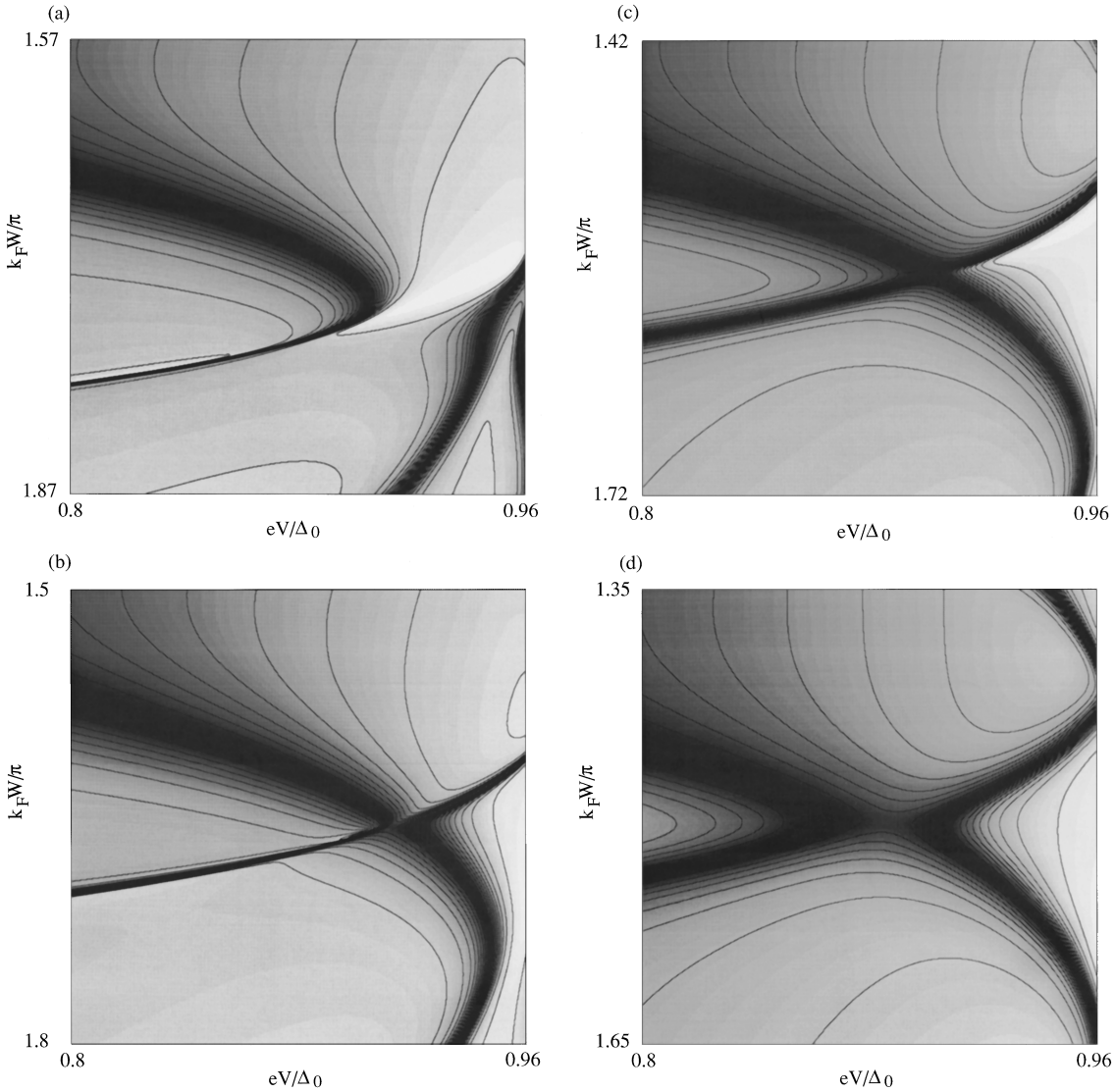

FIG. 11. Conductance G_{NS} as functions of $k_F W/\pi$ and eV/Δ_0 when D/W=(a) 2.4, (b) 2.6, (c) 2.8, and (d) 3.0. More conductive areas are brighter. For these results $\mu_S = 13E_1$ and $\Delta_0 = 0.02\mu_S$.

the ''poles.'' For $eV < \varepsilon_c$, the zero lies in the positive imaginary plane and the pole dominates the resonance characteristics. The zero reaches the real energy axis at $eV = \varepsilon_c$. Thus the peak in the transmission turns into a dip. The zero-pole pair splits into two zero-pole pairs for $eV > \varepsilon_c$. It is therefore concluded that the transmission amplitude is given by

$$t(E) \sim \frac{[E-(E_{ze}+i\gamma_e)][E-(E_{zh}+i\gamma_h)]}{[E-(E_{pe}-i\Gamma_e)][E-(E_{ph}-i\Gamma_h)]}. \qquad (20)$$

Here $\gamma_{e,h}=0$ for $eV > \varepsilon_c$ except when the anticrossing takes place. For the resonances at $k_F W/\pi = 1.48$ in Fig. 13(a), the poles are already separated while the zeros remain combined. This is consistent with the fact that the splitting of the conductance dip does not happen until the minimum conductance vanishes. The distance $\Gamma_{e,h}$ from the real energy axis to the pole adjacent to the threshold of the second mode is much smaller than that of the resonances at lower $k_F W/\pi$, accounting for the distinct width of the dips. When the zero-pole pairs originating from different quasibound states merge at the crossing point of the two resonance branches, the zero moves off the real energy axis in case of the anticrossing. As shown in Fig. 13(c), the separations between the zero and the pole are quite different when the zero-pole pairs associated with the narrow and broad dips meet, causing the complicated variation seen in Fig. 11.

IV. GREEN'S FUNCTION OF A ONE-DIMENSIONAL NS SYSTEM

Let us now use a simplified model of the NS system in order to clarify the mechanism of the peculiar behavior of the resonances. We can use the tight-binding lattice illustrated in the insets of Fig. 14 to extract the essence of the NS waveguide. The narrow semiconductor wire is modeled by a one-dimensional (1D) lead. The wide semiconductor and superconductor waveguides are, respectively, approximated by square lattices with M_N and M_S transverse lattice sites. We treat the tight-binding Hamiltonian

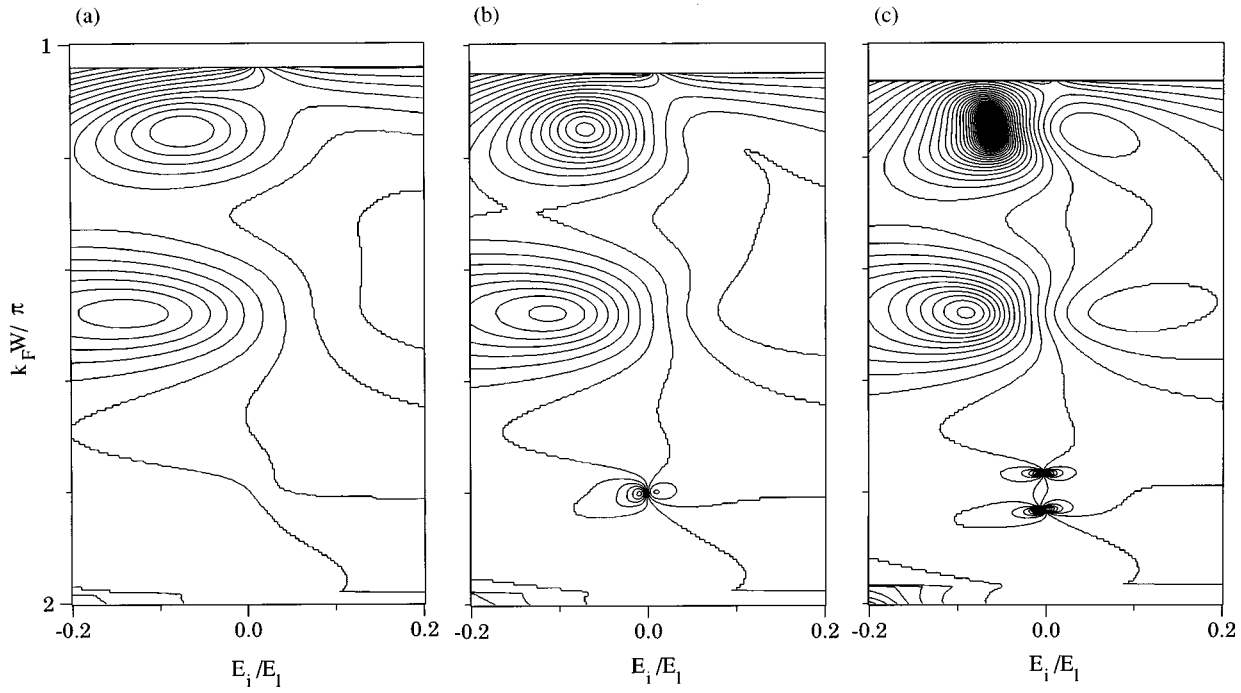

FIG. 12. Cantor plot of $\ln(G_{\rm NS})$ in the complex energy plane when the applied voltage is eV/Δ_0=(a) 0.3, (b) 0.4, and (c) 0.5. The width of the resonator region is D/W=2.6. Zeros and poles exist in the regions $E_i \geqslant 0$ and $E_i < 0$, respectively. $\mu_S = 13E_1$ and $\Delta_0 = 0.02\mu_S$.

$$H_{\rm TB} = -t\sum_{\rm NN}(c_i^+ c_j - d_i^+ d_j) - \sum_i \mu_i (c_i^+ c_i - d_i^+ d_i) + \sum_i (\Delta_i c_i^+ d_i + \Delta_i^* d_i^+ c_i), \tag{21}$$

where $c_i^+ (d_i^+)$ and $c_i(d_i)$ are the creation and annihilation operators of an electron (a hole) at the site $i=(l,m)$. The sum in the first term on the right-hand side is over nearest neighbors. We have calculated Green's function $G_{\rm NS} = \langle O|(\varepsilon - H_{\rm TB})^{-1}|O\rangle$.

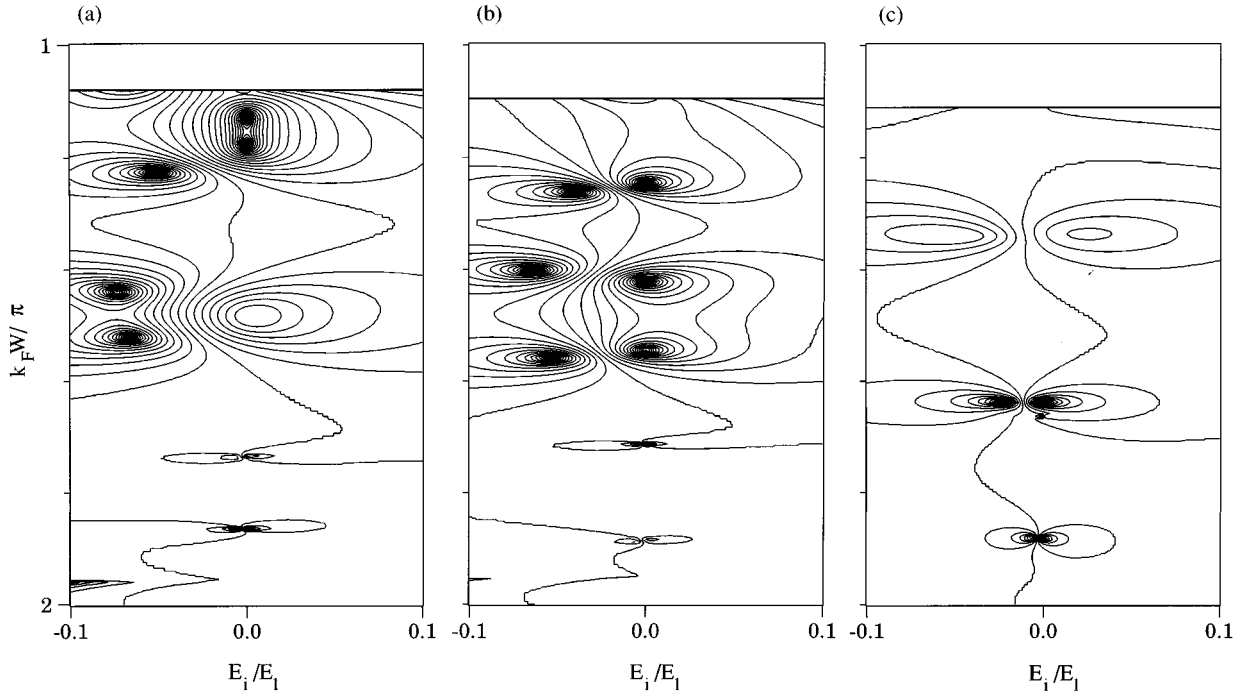

FIG. 13. Cantor plot of $\ln(G_{\rm NS})$ in the complex energy plane for eV/Δ_0=(a) 0.65, (b) 0.75, and (c) 0.9 when D/W=2.6. The increment of the curves is twice that in Fig. 12. Zero-pole pairs with small and large displacements between zero and pole, which correspond to the sharp and broad dips, are close in (c) at $k_F W/\pi \sim 1.65$. $\mu_S = 13E_1$ and $\Delta_0 = 0.02\mu_S$.

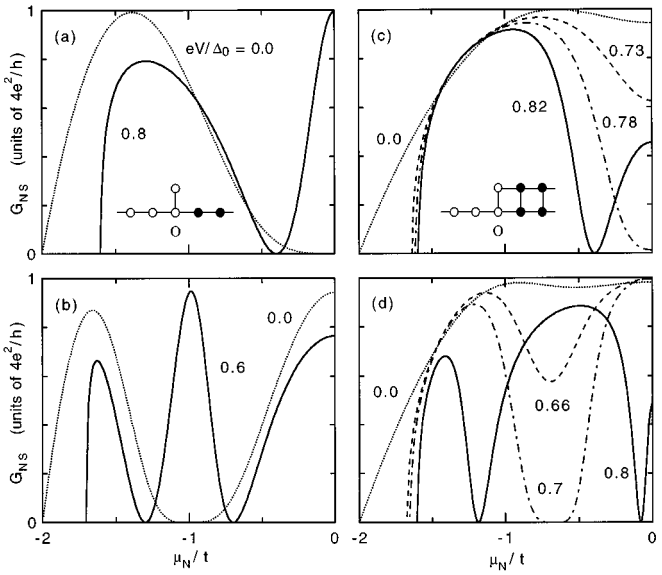

FIG. 14. Conductance G_{NS} as a function of the chemical potential μ_N in the normal-conductor for (a) $M_N=2$ and $M_S=1$, (b) $M_N=3$ and $M_S=1$, (c) $M_N=M_S=2$, and (d) $M_N=M_S=3$. The parameters in the superconductor are $\mu_S=0$ and $\Delta_0=0.5t$. Insets: Schematic of the tight-binding model of the NS system. The filled circles represent the superconducting sites, where the pair potential amplitude Δ_0 is assumed.

In the simplest case ($M_N=2$ and $M_S=1$), the off-diagonal component G_{he} of the 2×2 Green's-function matrix of the NS system, which is proportional to the reflection amplitude s_{he}, is

$$\mathrm{Re}\left[-\frac{g_{he}}{G_{he}}\right]=[\eta(\varepsilon+\mu)-tg_{ee}][\eta(\varepsilon-\mu)-tg_{hh}] + \frac{\chi(\varepsilon+\mu)\chi(\varepsilon-\mu)}{4}-t^2g_{he}^2, \tag{22a}$$

$$\mathrm{Im}\left[-\frac{g_{he}}{G_{he}}\right]=[\eta(\varepsilon-\mu)-tg_{hh}]\frac{\chi(\varepsilon+\mu)}{2} -[\eta(\varepsilon+\mu)-tg_{ee}]\frac{\chi(\varepsilon-\mu)}{2}, \tag{22b}$$

where $\eta(\varepsilon)=\varepsilon/2t-t/\varepsilon$ and $\chi(\varepsilon)=(4-\varepsilon^2/t^2)^{1/2}$. Here g_{ee}, g_{hh}, and g_{he} are the components of the Green's-function matrix of the 1D semi-infinite superconductor and are given in Appendix B. Therefore the resonant reflection always appears irrespective of ε at $\mu=-\varepsilon$, as shown in Fig. 14(a). For $M_N=3$ and $M_S=1$, $\eta(\varepsilon)$ is substituted by $\varepsilon/2t-t\varepsilon/(\varepsilon^2-t^2)$. The conductance now becomes zero when $\mu=-t\pm\varepsilon$. As the resonance is shifted lower in energy, the splitting of the dip for nonzero ε shows up as seen in Fig. 14(b). The resonance is, nevertheless, present for the entire range of values of ε ($0\leqslant\varepsilon\leqslant\Delta_0$). The behavior that the complete reflection at the resonance shows up only for $\varepsilon\geqslant\varepsilon_c>0$ is retrieved when $M_S=M_N\geqslant2$, as shown in Figs. 14(c) and 14(d). The resonance initially takes place at $\mu=0$ when $M_N=M_S=2$. When $M_N=M_S=3$, the NS system exhibits both the transition of a peak to a dip at finite ε_c ($=0.7$) and the splitting of the dip into electronlike and holelike dips.

V. SUMMARY

In conclusion, we have investigated the influence of Andreev reflection from the NS interface on the geometrical resonances in a waveguide structure. At zero applied voltage, the interference of the electronlike excitation exclusively gives rise to resonances as a consequence of the retroproperty of Andreev reflection. The normal reflection at the NS interface induced by the difference in the Fermi energies in the two materials is found to be reduced by utilizing the quantum interference effect in the semiconductor region. Despite the different appearance of the effects, i.e., improved conductance in the composite system contrary to the nearly zero conductance in the semiconductor NWN structure, the characteristics of the interference effect closely resemble those of the transmission resonances in the semiconductor counterpart. The fact that the current is carried by two kinds of quasiparticles in the NS system is particularly highlighted when a finite voltage is applied. The modulation pattern is altered like that when multimodes are occupied below the Fermi energy because of the different wave numbers for the electrons and the holes. With the finite voltage being applied to the NS junction, the retroproperty breaks down as the momenta of the incident electron and the Andreev-reflected hole can no longer be the same. Consequently, both the electron and the hole contribute to the resonances. The resonance induces sharp dips in the transmission when the voltage becomes larger than a critical value. We find that pairs of zeros and poles are generated in the complex energy plane for finite voltages. The resonance peaks observed at low voltages turn into nearly complete reflections as the zeros approach the real energy axis and take over the dominating role in the transmission properties. The zero-pole pair splits into electronlike and holelike zero-pole pairs, giving rise to the splitting of the dip in the transmission. We have shown that the interplay between the zero-pole pairs leads to the rich variety of behavior of the quantum interference effect in the NS system. In semiconductor waveguides, the electron and hole excitations cannot be interconverted to each other because of the absence of the coupling term. The resonances associated with the hole excitation are not relevant in the semiconductor counterpart.

APPENDIX A: CLASSICAL TRANSMISSION ALONG THE NS INTERFACE

We show here that the presence of Andreev reflection prevents transmission along the NS interface in the classical model. When a particle is incident on the NS interface it is, as shown in Fig. 15, either backscattered with probability p or specularly reflected with probability $1-p$. Flux conservation provides the relation

$$\begin{pmatrix} a_n \\ b_{n-1} \end{pmatrix}=\begin{pmatrix} 1-p & p \\ p & 1-p \end{pmatrix}\begin{pmatrix} a_{n-1} \\ b_n \end{pmatrix}, \tag{A1}$$

and the transfer matrix can be written as

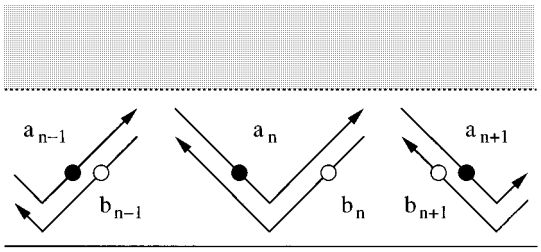

FIG. 15. Classical model of the propagation of the normal-reflected electron (filled circles) and the Andreev-reflected hole (open circles) along the NS interface.

$$\begin{pmatrix} a_n \\ b_n \end{pmatrix} = \begin{pmatrix} 1 & 1 \\ 1 & 1/p \end{pmatrix} \begin{pmatrix} 1 & 1 \\ 0 & 1 \end{pmatrix} \begin{pmatrix} 1 & 1 \\ 1 & 1/p \end{pmatrix}^{-1} \begin{pmatrix} a_{n-1} \\ b_{n-1} \end{pmatrix} = \begin{pmatrix} 1 & 1 \\ 1 & 1/p \end{pmatrix} \begin{pmatrix} 1 & n \\ 0 & 1 \end{pmatrix} \begin{pmatrix} 1 & 1 \\ 1 & 1/p \end{pmatrix}^{-1} \begin{pmatrix} a_0 \\ b_0 \end{pmatrix}. \quad \text{(A2)}$$

Therefore we obtain the scattering matrix as

$$\begin{pmatrix} a_n \\ b_0 \end{pmatrix} = \frac{1}{1-p+np} \begin{pmatrix} 1-p & np \\ np & 1-p \end{pmatrix} \begin{pmatrix} a_0 \\ b_n \end{pmatrix}. \quad \text{(A3)}$$

If the Andreev reflection probability is nonzero, the particle cannot propagate classically along the NS interface in an infinite system ($n \to \infty$).

APPENDIX B: GREEN'S FUNCTION IN THE NS SYSTEM

Here we calculate the Green's function of the 1D system. The recursion equation to obtain the Green's function of the semi-infinite 1D superconductor is

$$G_S^{1\mathrm{D}} = \begin{pmatrix} g_{ee} & g_{he} \\ g_{eh} & g_{hh} \end{pmatrix} = \begin{pmatrix} \varepsilon+\mu-t^2 g_{ee} & -\Delta_0+t^2 g_{he} \\ -\Delta_0+t^2 g_{eh} & \varepsilon-\mu-t^2 g_{hh} \end{pmatrix}^{-1}. \quad \text{(B1)}$$

It can be shown that

$$g_{ee} = \frac{1}{\alpha^2+\beta^2}\left(\alpha - \frac{\varepsilon\beta}{\sqrt{\Delta_0^2-\varepsilon^2}}\right), \quad \text{(B2a)}$$

$$g_{he} = g_{eh} = -\frac{\Delta_0\beta}{(\alpha^2+\beta^2)\sqrt{\Delta_0^2-\varepsilon^2}}, \quad \text{(B2b)}$$

$$g_{hh} = -\frac{1}{\alpha^2+\beta^2}\left(\alpha + \frac{\varepsilon\beta}{\sqrt{\Delta_0^2-\varepsilon^2}}\right), \quad \text{(B2c)}$$

where

$$\alpha = \frac{\mu}{2} + \frac{\mu\sqrt{\Delta_0^2-\varepsilon^2}}{\sqrt{2}[X+\sqrt{X^2+4\mu^2(\Delta_0^2-\varepsilon^2)}]^{1/2}},$$

$$\beta = \frac{\sqrt{\Delta_0^2-\varepsilon^2}}{2} + \frac{[X+\sqrt{X^2+4\mu^2(\Delta_0^2-\varepsilon^2)}]^{1/2}}{2\sqrt{2}},$$

$$X = 4t^2+\Delta_0^2-\varepsilon^2-\mu^2.$$

$G_S^{1\mathrm{D}}$ is real because there is no propagating mode when $\Delta_0 > \varepsilon$. The Green's function of the 1D normal conductor is

$$G_N^{1\mathrm{D}} = \frac{1}{2t^2}\begin{pmatrix} \varepsilon+\mu-i\sqrt{4t^2-(\varepsilon+\mu)^2} & 0 \\ 0 & \varepsilon-\mu+i\sqrt{4t^2-(\varepsilon-\mu)^2} \end{pmatrix}. \quad \text{(B3)}$$

By attaching a single semiconductor site and the 1D superconductor lead to the 1D semiconductor lead, it is shown that the Green's function G_{NS} of the NS system with $M_N=2$ and $M_S=1$ satisfies

$$G_{\mathrm{NS}}^{-1} = G_N^{-1} - t^2 P\left[G_S + \begin{pmatrix} 1/(\varepsilon+\mu) & 0 \\ 0 & 1/(\varepsilon-\mu) \end{pmatrix}\right] P. \quad \text{(B4)}$$

The off-diagonal component of G_{NS} is given by Eq. (22). For $M_N=M_N=2$, the NS system can be constructed by assembling the 1D semiconductor lead, connected two semiconductor sites (which are represented by the Green's function g_0), and a superconductor strip. The Dyson equation yields

$$G_{\mathrm{NS}}^{-1} = g_0^{-1} - t^2 P(G_N+G_S)P. \quad \text{(B5)}$$

Taking into account the symmetry of the superconductor strip, we can express the 4×4 matrix G_S as $(G_S)_{11}=(G_S)_{22}=g_1$, $(G_S)_{13}=(G_S)_{24}=(G_S)_{31}=(G_S)_{42}=g_2$, $(G_S)_{33}=(G_S)_{44}=g_3$, $(G_S)_{12}=(G_S)_{21}=g_4$, $(G_S)_{34}=(G_S)_{43}=g_5$, and $(G_S)_{14}=(G_S)_{23}=(G_S)_{32}=(G_S)_{41}=g_6$ with g_i being real. Notice that all the components of this matrix are nonzero when all the sites in the wide semiconductor region are in contact with the superconducting sites, i.e., $M_N=M_N$. We find that the zeros of the response G_{he} of a hole at the site O (see the inset in Fig. 14) due to an injection of an electron at that site is given as the zeros of a polynomial of degree two (neglecting the μ dependence of g_i). It can be proved that when $\varepsilon=0$ $G_{he}\neq0$ for real μ. One may construct the NS system with $M_N=2$ and $M_S=1$ in the latter manner. It is shown that $G_{he}=-t^2 g_2(\varepsilon^2-\mu^2)/D$, where D is the determinant of the 4×4 matrix G_{NS}^{-1}. Since many components of G_S are zero, $G_{he}=0$ is found to be achieved at $\mu=0$ when $\varepsilon=0$.

ACKNOWLEDGMENT

The authors wish to thank S. Tarucha for valuable comments.

[1] P. L. McEuen, E. B. Foxman, U. Meirav, M. A. Kastner, Y. Meir, and N. S. Wingreen, Phys. Rev. Lett. **66**, (1991).
[2] Y. Takagaki and D. K. Ferry, Phys. Rev. B **45**, 13 494 (1992).
[3] F. Sols, M. Macucci, U. Ravaioli, and K. Hess, Appl. Phys. Lett. **54**, 350 (1989).
[4] Y. B. Levinson, M. I. Lubin, and E. V. Sukhorukov, Phys. Rev. B **45**, 11 936 (1992).
[5] P. J. Price, Phys. Rev. B **38**, 1994 (1988).
[6] P. J. Price, Appl. Phys. Lett. **62**, 289 (1993).
[7] W. Porod, Z. Shao, and C. S. Lent, Appl. Phys. Lett. **61**, 1350 (1992).
[8] L. D. Landau and E. M. Lifshitz, *Quantum Mechanics* (Pergamon, Oxford, 1977), Sec. 134.
[9] H. Takayanagi, J. B. Hansen, and J. Nitta, Phys. Rev. Lett. **74**, 166 (1995); H. Takayanagi, T. Akazaki, and J. Nitta, *ibid*. **75**, 3098 (1995); H. Takayanagi and T. Akazaki, Phys. Rev. B **52**, R8633 (1995).
[10] For a review, see C. W. J. Beenakker, in *Mesoscopic Quantum Physics*, edited by E. Akkermans, G. Montambaux, and J.-L. Pichard (North-Holland, Amsterdam, in press).
[11] A. F. Andreev, Zh. Eksp. Teor. Fiz. **46**, 1823 (1964) [Sov. Phys. JETP **19**, 1228 (1964)].
[12] G. E. Blonder, M. Tinkham, and T. M. Klapwijk, Phys. Rev. B **25**, 4515 (1982).
[13] C. W. J. Beenakker, Phys. Rev. B **46**, 12 841 (1992).
[14] I. K. Marmorkos, C. W. J. Beenakker, and R. A. Jalabert, Phys. Rev. B **48**, 2811 (1993).
[15] K. K. Likharev, Rev. Mod. Phys. **51**, 101 (1979).
[16] T. Ando, Phys. Rev. B **44**, 8017 (1991).
[17] The transmission modes in a semiconductor wire contain the oscillatory dumped modes, for which $(k_n W)^2$ is complex, in the presence of a magnetic field. See R. L. Schult, H. W. Wyld, and D. G. Ravenhall, Phys. Rev. B **41** 12 760 (1990).
[18] A. Kumar and P. F. Bagwell, Phys. Rev. B **44**, 1747 (1991).
[19] Y. Takagaki and D. K. Ferry, Phys. Rev. B **45**, 6715 (1992).
[20] Y. Takane and H. Ebisawa, J. Phys. Soc. Jpn. **61**, 1685 (1992).
[21] C. J. Lambert, J. Phys.: Condens. Matter **3**, 6579 (1991).
[22] P. F. Bagwell, Phys. Rev. B **46**, 12 573 (1992).
[23] Y. Takagaki and D. K. Ferry, Phys. Rev. B **44**, 8399 (1991).
[24] Y. Takagaki and H. Takayanagi, Phys. Rev. B **53**, 14 530 (1996).
[25] B. J. van Wees, P. de Vries, P. Magnée, and T. M. Klapwijk, Phys. Rev. Lett. **69**, 510 (1992); H. Takayanagi, E. Toyoda, and T. Akazaki (unpublished).
[26] F. Sols, M. Macucci, U. Ravaioli, and K. Hess, J. Appl. Phys. **66**, 3892 (1989).
[27] The conductance in Fig. 9 shows upward cusp when $eV=0.5\Delta_0$, while drops discontinuously when $eV=0.7\Delta_0$. The singularities at the mode threshold have been studied by H. U. Baranger, Phys. Rev. B **42**, 11 479 (1990).
[28] W. Porod, Z. Shao, and C. S. Lent, Phys. Rev. B **48**, 8495 (1993).
[29] T. B. Bahder, C. A. Morrison, and J. D. Bruno, Appl. Phys. Lett. **51**, 1089 (1987).